ORIGINAL ARTICLE

lajss.org© Latin American Journal of Solids and Structures

www.lajss.org

Numerical model for analysis of compact and slender hybrid steel beams subjected to bending

Caroline Martins Calisto[a]*, Ana Lydia Reis de Castro e Silva[a], Rodrigo Barreto Caldas[a], Hermes Carvalho[a,b]

[a] Departamento de Engenharia de Estruturas, Universidade Federal de Minas Gerais, Belo Horizonte, MG, Brasil. Email: carolinemartinscalisto@yahoo.com.br, analydiarcs@gmail.com, rbcaldas@gmail.com, hermes@dees.ufmg.br
[b] Departamento de Engenharia de Estruturas e Geotécnica, Universidade de São Paulo, São Paulo, SP, Brasil.

* Corresponding author

https://doi.org/10.1590/1679-78257411

Abstract

This article presents a study of the behavior of hybrid steel beams of I-profile cross section subjected to bending. Numerical models of finite elements were developed and validated in the ABAQUS software. In the models, lateral buckling with torsion was disregarded, since the beam will be laterally restrained, so that only local instabilities are present and thus evaluated. Analyses were divided into two stages: first, the elastic buckling analysis was carried out to obtain the critical buckling loads and the buckling modes of the beams; subsequently, analysis of the ultimate strength capacity of the beams was carried out considering residual stresses and initial imperfections. The numerical model was defined and a sensitivity study of the yield strength of the flange steel was carried out. The obtained results from the developed numerical model were satisfactory and, as expected, showed that the hybrid beams resist a greater bending moment effort when compared to their corresponding homogeneous beams.

Keywords

Hybrid steel beams, local instability, I profile, nonlinear analysis.

Graphical Abstract

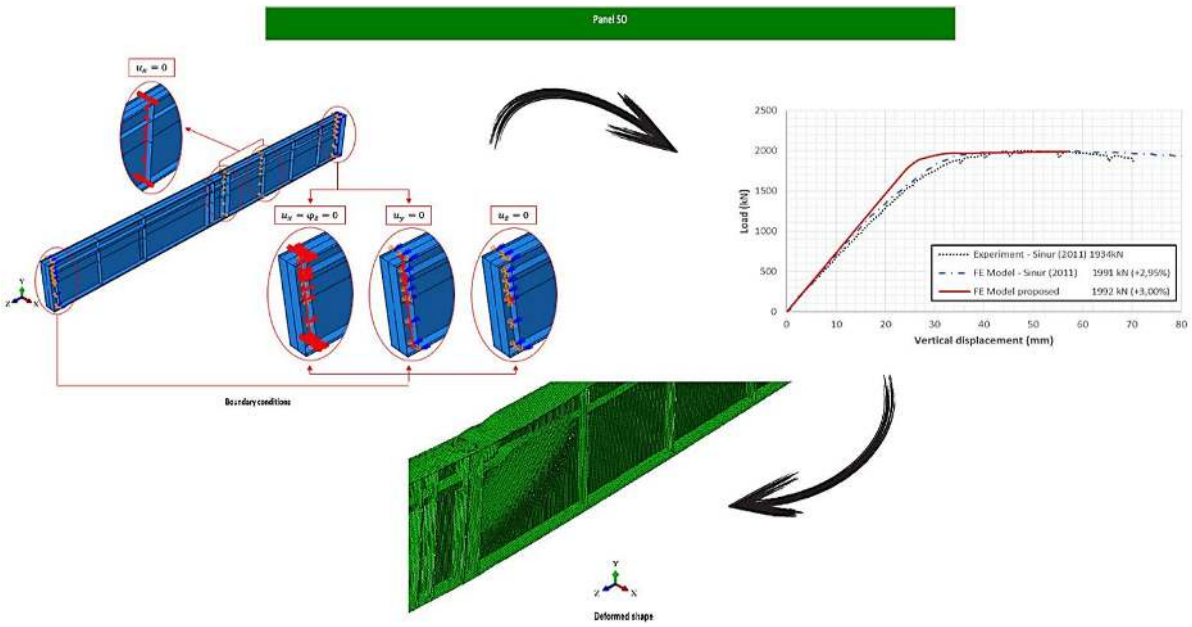

Received December 15, 2022. In revised form April 14, 2023. Accepted April 24, 2023. Available online April 27, 2023.
https://doi.org/10.1590/1679-78257411

Latin American Journal of Solids and Structures. ISSN 1679-7825. Copyright © 2023. This is an Open Access article distributed under the terms of the Creative Commons Attribution License, which permits unrestricted use, distribution, and reproduction in any medium, provided the original work is properly cited.

1 INTRODUCTION

According to Chacón (2009), high-strength steel provides new options for structural design, but there is a mismatch between the scientific and technological advances and the practical application, due to the lack of standards for these steel types. In Europe, EN 1993-1-12:2007 was only recently created, which specifies the uses of steel in the S460 - S700 range.

On the other hand, the advantages of using high strength steel are increasingly notable, and one of its applicability refers to hybrid beams. In this type of beam, the I-profile beam is welded and has different types of steel in the flanges and in the web and, in most cases, the flanges are composed of a higher strength steel. According to Beg et al. (2010), hybrid beams are considered an inexpensive solution, as the most resistant and, therefore, the most expensive material (high-strength steel) is only used in the most requested locations of the profile.

According to Gogou (2012), when comparing hybrid designs and their equivalent homogeneous designs for the 'Schellingwouderbrug' bridge, located in the Netherlands, it was proven that hybrid designs resulted in weight savings of up to 65%. The high-cost of high strength steels results in a higher cost for hybrid projects, around 4%. However, the weight reduction in these projects is quite significant, which leads to a reduction in the total cost, up to 6% lower, considering manufacturing, transport, assembly and maintenance.

Therefore, the use of hybrid beams is associated with cost reductions and the fact that they are lighter than conventional beams. Research carried out in other countries has shown that this subject is relevant and provides proven benefits. This hybrid design has been employed on bridges in the United States, Europe, and Japan. In Brazil, this topic is little discussed and lacks research and its own regulations, which encourages the research on this type of solution.

To make it possible to carry out broader research on the subject, it is necessary to conduct parametric studies, statistical analyses, and to define equations for dimensioning profiles, among other investigations. For that, it is crucial to obtain a reliable numerical model calibrated by an experimental model.

This article seeks to contribute in this field of study by developing, implementing and testing a numerical model on ABAQUS, a software capable of satisfactorily representing compact and slender hybrid steel beams with or without stiffeners.

A numerical model was developed according to previously conducted studies. Shokouhian (2014) studied the ductility and ultimate strength of bent beams. In addition to the theoretical analysis, the author addressed experimental and numerical tests of these beams using the finite element program ANSYS 14.5. Sinur (2011) investigated the behavior of four panels of two transversely and longitudinally stiffened beams subjected to bending and shear through experimental, numerical, and theoretical analyses. One beam has a symmetrical cross section with one rectangular and one trapezoidal stiffener and the other beam has an asymmetrical cross section with two rectangular and one trapezoidal stiffener. For this study only panels with rectangular stiffeners were considered, therefore, only one panel of each beam was analyzed.

It was decided to validate the slender numerical model based on the research of Sinur (2001), as it has a broader and more detailed study material of the bending of slender beams with stiffeners, even though it is not a specific research of hybrid beams.

From the study of the art of hybrid beams conceived by Chacón (2009) and improved 5 years later by Chacón (2014) and the research by Kulkarni and Gupta (2017), Table 1 was developed by Chacón (2014) and adapted to present the research involving the use of high strength steels in beams in a chronological scheme.

Taking these three previous studies of hybrid beams into account, the main researches related to the subject will be described and Table 1 will include some other intermediate researches that were also carried out.

The first hybrid design proposal was presented in North America by Wilson in 1944. His investigation was based on a solution related to the weight and material cost of a beam with carbon steel in the web and silicon steel in the flanges. However, it was only in 1961 that this concept was reintroduced into research by Haaijer in his research on high strength profiles.

Later, in 1964, Frost and Schilling presented a more complete research that encompassed the theoretical and experimental field on the behavior of hybrid steel beams under pure bending moment and under the combination of moment and shear, developing graphs of the bending moment versus rotation correlation. It is considered that the first rules for designing hybrid beams by AASHTO in 1968 were based on this work. The only records found on programming hybrid beams date from 1976, 1986 and 1987. According to Abuyounest and Adeli (1987), in 1976 the author Chong studied the optimization of hybrid beams without stiffening considering the lowest optimization cost for moment and shear. In 1986, Adeli and Phan (1986) developed a software for designing welded hybrid and non-hybrid beams according to the 1980 AISC standard.

Table 1: Researches related to hybrid beams with I-profile cross-section arranged chronologically (adapted from Chacón, 2014).

Researchers	Year	Base	Topic
Wilson	1944	T	First report
Haaijer	1961	T	HSS
Frost and Schilling	1964	T and E	Bending and shear
Sarsam	1966	T and E	Bending and shear
Schilling	1967	T and E	Patch loading
Lew and Toprac	1967	T and E	Bending and shear
Schilling	1968	T	Composite hybrid girder
Carskaddan	1968	T and E	Shear buckling
Maeda	1971	T and E	Bending resistance
Nethercot	1976	T and E	Shear buckling
Chong	1976	-	Programming
Adeli and Phan	1986	-	Programming
Abuyounest and Adeli	1987	-	Programming
Åhlenius	1994	General	Design
Axhag	1998	E	Bending resistance
Barker and Schrage	2000	Economy	Economical advantages
Rush	2001	E	Shear capacity
Barker et al.	2002	T	Shear capacity
Zentz	2002	E	Shear capacity
Greco and Earls	2003	T and N	Bending resistance
Bitar et al.	2003	T, E and N	Bending resistance
Veljkovic and Johansson	2004	Economy, N and E	Design
Ito et al.	2005	T, E and N	Bending resistance
Johansson and Collin	2005	Economy	Economical advantages
Barker et al.	2005	E	Shear capacity
Fenkel et al.	2007	T, E and N	Lateral buckling
Barth et al.	2007	N	Bending resistance
Azizinamini	2007	E	Shear capacity
Projeto COMBRI	2008	T, E and N	Design
Petel et al.	2008	Economy	Weight savings
Real et al.	2008	E	Shear capacity
Chacón et al.	2009	T, E and N	Patch loading
Chacón et al.	2010	T and N	Patch loading
Ajeesh	2011	T	Shear capacity
Chacón et al.	2011	T and N	Patch loading
Gogou	2012	Economy	Design alternatives
Chacón et al.	2012	N	Patch loading
Chacón et al.	2013	N and E	Patch loading
Rojas Blonval	2013	T and N	Shear capacity
Chacón	2014	T	State-of-the-art
Shokouhian and Shi	2014	T and N	Bending resistance
Shokouhian and Shi	2015	T and E	Bending resistance
Chacón and Rojas-Blonval	2015	N	Shear capacity
Shokouhian et al.	2016	T and E	Failure modes
Wang et al.	2016	T, E and N	Bending resistance
Subramanian and White	2016	T and N	Bending resistance
Kulkarni and Gupta	2017	T, E and N	Bending resistance
Ghadami and Broujerdian	2018	T and N	Bending resistance and shear capacity
Shokouhian et al.	2018	T and E	Bending resistance and shear capacity
Lalthazuala and Singh	2019	N	Bending resistance
Biscaya et al.	2019	E and N	Bending resistance and shear capacity
Khartode et al.	2020	N	Bending resistance
Khartode et al.	2020	N	Shear capacity

Later, Abuyounest and Adeli (1987) presented a minimum weight design for hybrid beams with or without stiffening, subjected to an arbitrary load from an implementation in the FORTRAN software. Barker and Schrage (2000) researched the benefits of high strength steel in beams for a bridge when analyzing six alternatives. In conclusion, the hybrid project presented more benefits, such as a lighter and cheaper structure. In contrast, although homogeneous beams composed by HPS present a significant reduction in weight, the cost of this material outweighs the benefits of having a lighter structure.

A project was carried out to verify the cross-sectional class, bending moment resistance, shear strength, transverse forces and fatigue, whose results were presented by Bitar et al. in 2003, Veljkovic and Johansson (2004) and Johansson and Collin (2005). With this, Chacón (2009) concluded that the design of hybrid beams can be performed using the rules for designing homogeneous beams according to EN 1993-1-5:2006, albeit with some modifications.

Ajeesh (2011) carried out a research based on the shear strength of hybrid beams in relation to some parameters such as, for example, slenderness. In the year 2012, Gogou (2012) compared the base cost for preliminary design alternatives for the 'Schellingwouderbrug' bridge and concluded that hybrid girders (combination of S355 and S690 steels) led to a more economical solution when comparing to a bridge with an equivalent homogeneous beam with S355 in its entire section. Shokouhian and Shi (2014), Shokouhian and Shi (2015) and Shokouhian et al. (2016) presented theoretical, analytical and experimental results on rotation capacity, ductility and failure modes of hybrid beams, and lastly, empirical equations were suggested. Also in 2015, Chacón and Rojas-Blonval (2015) presented an analysis of hybrid beams subject to shear forces. In 2013, Rojas-Blonval (2013) had already investigated shear instability in hybrid beams.

Wang et al. (2016) studied thirteen hybrid beams and concluded that the slenderness of the flange or web is the main factor affecting the bending capacity and ductility of a beam. Later, Kulkarni and Gupta (2017) performed bending tests on five beams with I-profile cross-section, two of them being homogeneous beams and the other three being hybrid beams. The hybrid beams were only tested for static loads and some suggestions were made for the EN 1993-1-1:2005 standard. Subramanian and White (2016) evaluated the contribution of a longitudinal stiffener in the ultimate yield state of flexural strength in hybrid and homogeneous slender steel beams. Based on the results, the authors recommended a cross-sectional model that captures the post-buckling response of the web for both types of beams subject to uniform moment.

Ghadami and Broujerdian (2018) theoretically and experimentally investigated the interaction between moment and shear in the behavior of hybrid beams at environmental temperature and at elevated temperatures. As a result, the authors proposed theoretical equations to attain the moment versus shear interaction curve without taking shear buckling into consideration. Shokouhian et al. (2018) investigated the interaction of buckling modes of hybrid beams with I-profile cross section subjected to bending, in which a slenderness-based method is presented to address the ductility and moment capacity affected by local and global instabilities.

More recently, Biscaya et al. (2019) addressed the interaction between moment and shear of longitudinally compressed and stiffened hybrid beams, however, in the analyzed cases, the flanges have a lower resistance steel than the web. Lalthazuala and Singh (2019) presented numerical studies on three types of beams, one of them being hybrid beams subject to bending.

In October 2020, Khartode et al. (2020) conducted a finite element analysis investigation of hybrid steel beams of I-profile cross sections with different locations of stiffeners with support on ANSYS software. The main objective was to achieve cost reduction and increase the load capacity of the beams. The authors concluded that when using stiffeners, the strength and bending of the beam increase, however, the bending at a slower rate. Furthermore, they also concluded that beams with vertical stiffeners have higher stiffness than beams with longitudinal stiffeners. In November of the same year, Khartode et al. (2020) carried out a parametric study on hybrid steel beams and concluded that the design of this type of beam uses parameters such as aspect ratio, web slenderness and the ultimate shear strength increases as the steel grade increases. Furthermore, the authors determined the bending of hybrid steel beams by varying the yield stress of the steel both in the web and in the flanges of the I-profile beam.

In addition to researches on hybrid beams, it is also important to highlight some recent and important studies on columns and beam-columns that use high-strength steels *e.g.,* Su et al. (2021) and Filho et al. (2022).

Filho et al. (2022) carried out an experimental and numerical study to investigate the behavior of columns of I-profiles welded with S690 steel failing by buckling due to flexion around the major and minor inertia axis, and column beams failing by lateral buckling with torsion. They concluded that EN 1993-1-1:2005, EN 1993-1-12:2007, ANSI/AISC 360-16 and AS 4100-2016 exhibited conservative results against strengths obtained in the experimental analysis.

2 DEVELOPMENT AND VALIDATION OF NUMERICAL MODELS

During the analyses, the ABAQUS program (SIMULIA, 2014) was utilized for the elaboration of three numerical models based on the Finite Element Method (FEM). The first model refers to compact beams. The second and third are

related to slender beams with one and two longitudinal stiffeners, respectively. It is important to note that all models are contained laterally. The same analysis procedure was adopted for the proposed models. First, an elastic buckling analysis was carried out to obtain the critical buckling loads and an approximation of the buckling modes of the beams. Then, an analysis of the ultimate strength capacity was carried out according to the approximation of the first buckling mode. In this last analysis the introduction of residual stresses and initial geometric imperfections in the compact model was considered, while in the slender models only the initial geometric imperfections were considered.

More specifically, this topic seeks to detail the development of numerical models, validate numerical and experimental models obtained by Shokouhian (2014) and Sinur (2011) and, finally, propose numerical models for carrying out parameter variation researches. There are three numerical models with the same characteristics of load application, boundary conditions, etc. so that it is possible to reach a general numerical model.

2.1 Description of modeling procedures

Six compact simply supported beams of I-profile cross section subjected to two concentrated loads were analyzed, three of them being conventional (C1, C2 and C3) and the other three being hybrid (H1, H2 and H3). The loads are located in thirds of the length of the beam, which generates a constant bending moment in the central region of the beam.

The distance between the supports (L) that guarantee the condition of a simply supported beam is 3 meters, with an additional length corresponding to L/15 on both ends, modeled with the same dimensions as the beam. Four vertical stiffeners are considered on each side of the web, two of which are located in the support reactions and the other two at the points of application of concentrated loads, aiming the prevention of occurrence of instability due to localized compression in the web, as can be seen be observed on Figure 1.

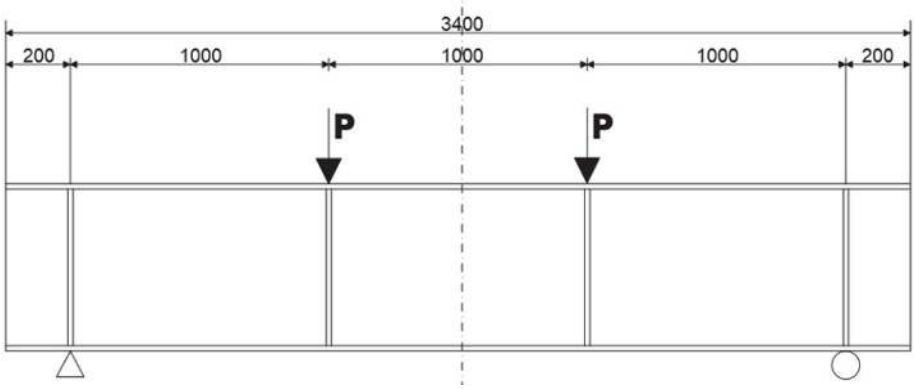

Figure 1: Geometric specification of the numerical model (Shokouhian, 2014).

The dimensions were considered in the mean plane of the cross section of the six beams, and the yield strength of the flanges and web were adopted according to the author's experimental analysis, as presented in Table 2, where b_{fb} is the width of the lower flange; b_{fu} the width of the upper flange; *h* is the height of the web; *h'* the height of the web considering the mean plane of the cross section; t_{fb} the thickness of the bottom flange; t_{fu} the thickness of the upper flange; t_w is the thickness of the web; f_{yf} the yield strength of the flange steel and f_{yw} the yield strength of the web steel.

Table 2: Considered dimensions of the beams for the analysis of compact models.

Model	h' (mm)	t_w (mm)	b_{fu} (mm)	t_{fu} (mm)	b_{fb} (mm)	t_{fb} (mm)	f_{yf} (N/mm²)	f_{yw} (N/mm²)
C1	369.30	7.87	169.00	11.91	170.20	11.89	408.20	442.80
C2	370.34	7.82	263.60	11.85	263.80	11.87	408.20	442.80
C3	610.34	7.94	168.20	11.75	168.60	11.77	408.20	442.80
H1	371.08	7.83	168.20	12.56	168.00	12.60	545.10	442.80
H2	371.59	7.79	264.80	12.68	263.60	12.57	545.10	442.80
H3	610.77	7.93	167.00	12.63	168.00	12.63	545.10	442.80

The stiffeners are continuous along the entire height of the web and have a thickness equal to 14 mm in all analyses, so that their width and height vary according to the width of the flange and the height of the web of each beam.

The elasto-plastic behavior of a structural steel was adopted according to the author's experimental study and, as shown in Figure 2, with an elastic zone and two plastic zones. For a steel with f_y = 408.20 N/mm^2: longitudinal modulus of elasticity (E) = 178.50 GPa, f_u= 529.50 N/mm^2, $\varepsilon_{st}/\varepsilon_y$ = 4.77 and $\varepsilon_u/\varepsilon_y$ = 33.99. For a steel with f_y = 442.80 N/mm^2: E = 197.60 GPa, f_u = 555.30 N/mm^2, $\varepsilon_{st}/\varepsilon_y$ = 8.06 and $\varepsilon_u/\varepsilon_y$ = 38.45. Lastly, for a steel with f_y= 545.10 N/mm^2: E = 206.80 GPa, f_u = 627.20 N/mm^2, $\varepsilon_{st}/\varepsilon_y$ = 11.45 and $\varepsilon_u/\varepsilon_y$ = 32.80. Poisson's coefficient (υ) equaled to 0.3. After failure, it was considered that the stress returns to a value very close to zero so that it would be possible to observe more clearly the ultimate strength capacity of the beam.

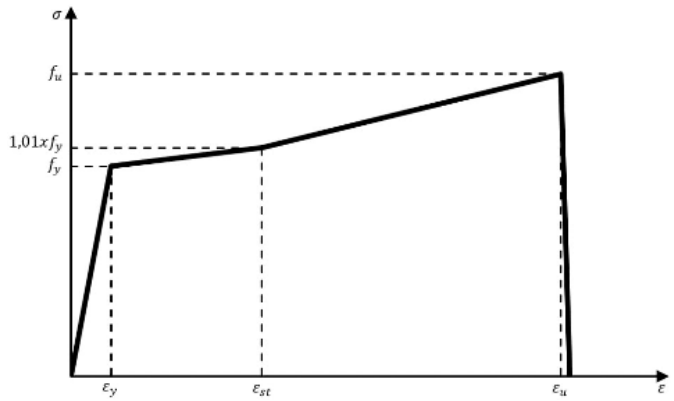

Figure 2: Stress x elastic-plastic strain diagram adopted in the analysis of compact models.

The axis system was defined in such a way that the Z axis corresponds to the longitudinal direction of the beam, while the x and y axes represent the largest and smallest axis of inertia, respectively. To ensure the expected behavior, the translations on the x (u_x) and y (u_y) axes were constrained, as well as the rotations around y (φ_y) and z (φ_z) axes along the junction between the lower flange and the transverse stiffener at both ends of the beam. In addition, the translation on the z axis (u_z) at one of the ends was also constrained. In order to concentrate the influences of local instabilities on the behavior of the beam, the numerical models were also constrained in terms of the out-of-plane translation of the web along the junction between the web and the upper flange of the profile, as shown in Figure 3.

A pressure-type distributed load applied to two solids was adopted, which were called loading plates, as observed in Figure 3. Each loading plate has a length equal to the width of the upper flange of the profile, a thickness of 20 mm and a width of 50 mm.

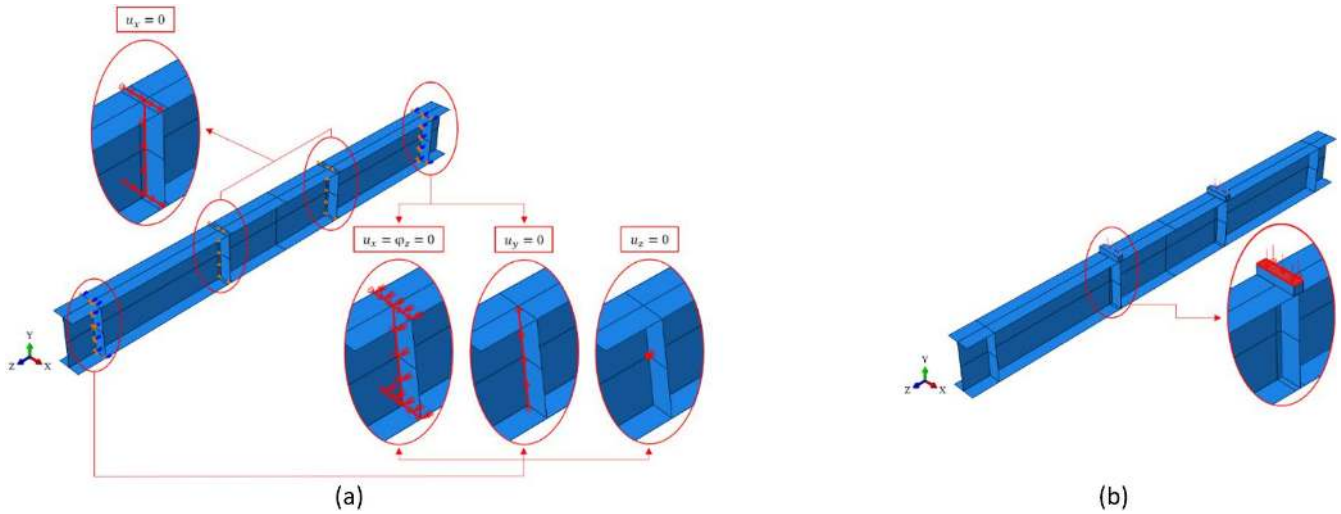

Figure 3: Compact model: boundary conditions and (b) detail of the distributed load applied to the I-profile.

The junction between the I-profile beam and the loading plates was carried out through the tie-type restriction. With this type of constrain, it was possible to connect the two surfaces and prevent the relative movement between them.

It is known that the initial imperfections are present in the plates that make up the profile. However, an analysis was carried out beforehand to compare the behavior of the beam when initial imperfections are present and when they are absent.

Therefore, as Shokouhian (2014) did, to introduce the initial geometric imperfection, a linearized stability analysis that was initially carried out to obtain the eigenvalue (critical buckling load) and the eigenvector (deformed configuration), from that it was observed the largest displacement, according to the relevant failure mode, and the imperfection value measured by the author was applied considering the failure mode - the maximum value measured by LVDT among five cross sections of the profile - throughout the model and, although the ideal scenario would be to adopt a distribution of residual stresses for conventional beams and another one for hybrid beams, due to the lack of data on the distribution of residual stresses in this second case, the author adopted the distribution of residual stresses proposed by Ban et al. (2013). It should be noted, however, that the experimental researches by Ban et al. (2013) were performed only on conventional beams composed of the same steel, as can be seen in Figure 4. The S4R element was chosen, a type of shell element with reduced integration that has four nodes.

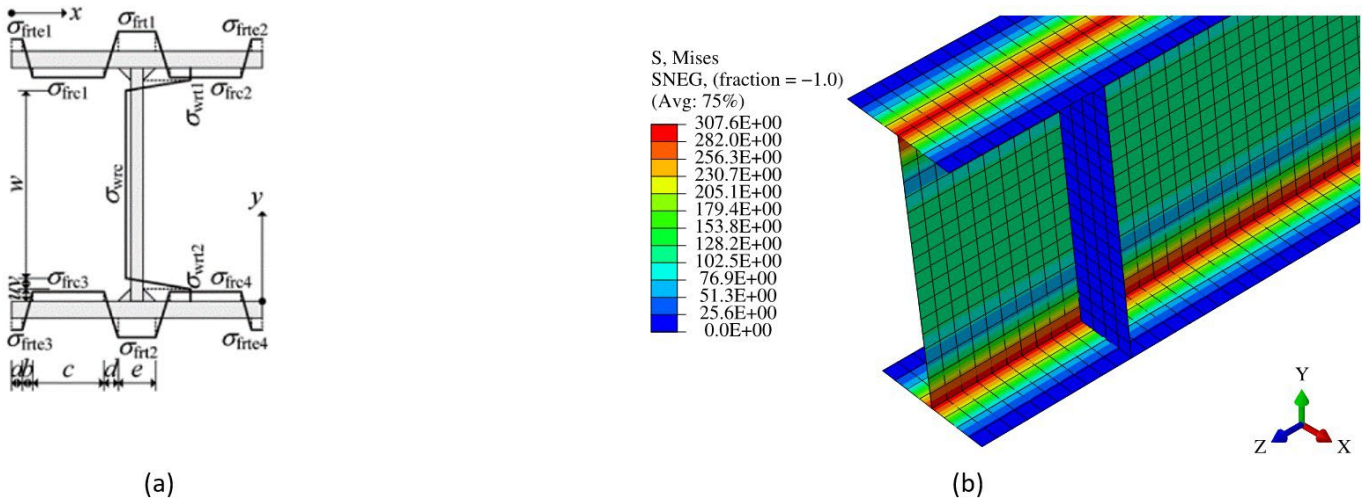

Figure 4: Residual stresses: (a) distribution of residual stresses (Ban et al., 2013) and (b) residual stress applied to numerical model C1.

It is known that the use of a finer mesh of finite elements generally provides a better approximation of the numerical model when compared to the use of a coarser mesh. The author did not mention the dimension of the finite elements adopted in the models, a mesh sensitivity study was carried out with elements of approximately 10 mm, 15 mm, 20 mm, 25 mm and 30 mm. Considering the bending moment curve (M) versus rotation (θ) and the correlation between the processing time of each numerical model (t_p) and the processing time of the model of reference (t_r), taken as the processing time of the model with elements mesh of approximately 10 mm, the average dimension of the finite elements was defined as equal to 20 mm in the I-profile and 5 mm in the loading plates.

For example, Figure 5 depicts the final deformation of beam C3. Due to the fact that the height of the web is greater than the height of the web of beam C1, local buckling of the web occurred, which induced local buckling of the flange. Two semi-waves were observed in the webs in the two final panels, and lastly the local buckling of the flange occurs in the central part of the beam.

For the slender panels, two I-profile cross-section beams were analyzed. The first beam has a symmetric cross section and a length of 11.16 m. The second beam has an asymmetric cross section and a length of 11.35 m. Both have rectangular and trapezoidal longitudinal stiffeners, however, this research addresses only one panel in each of the beams, and the panels analyzed in both are the panels with the presence of rectangular longitudinal stiffeners.

The symmetric beam has a rectangular longitudinal stiffener and a trapezoidal stiffener. Their center of gravity is positioned in the compressed zone of the web, 350 mm from the upper flange. There are seven intermediate transverse stiffeners with a thickness of 15 mm and a width of 120 mm, and six double transverse stiffeners with a thickness of 20 mm and a width of 156 mm. Dual transverse stiffeners were used in the core of the beam to apply the external load. They were also used after the additional length of the supports to secure the rigid end of the beam. Furthermore, outside the investigation area — 120 mm from the intermediate transverse stiffeners — the web thickness is 8 mm and only in the core of the beam (at the length of 800 mm). The author considered the web thickness equal to 15 mm to ensure elastic behavior in this transition area. For this article, the SO panel of the beam was analyzed, which has a rectangular longitudinal stiffener.

The asymmetrical beam has two rectangular longitudinal stiffeners and one trapezoidal stiffener and, as in the symmetrical beam, the center of gravity of the first rectangular longitudinal stiffener and the trapezoidal stiffener are located 350 mm from the upper flange. The second rectangular longitudinal stiffener is located 350 mm from the center of gravity of the first rectangular longitudinal stiffener. There are six intermediate transverse stiffeners 20 mm thick and 122 mm wide and six double transverse stiffeners 20 mm thick and 122 mm wide located in the same manner as the previous beam. Outside the investigation area — 120 mm from the intermediate transverse stiffeners — the web thickness is 7 mm and, as in the previous beam, a web thickness equal to 15 mm was considered in the central part of the beam. In this beam, the UO panel was analyzed, which has two rectangular longitudinal stiffeners. The trapezoidal longitudinal stiffener has a width equal to 90 mm on the symmetric beam, a thickness equal to 10 mm, and a length equal to 5675 mm. As for the asymmetric beam, the trapezoidal longitudinal stiffener has a width equal to 100 mm, a thickness equal to 10 mm and a length equal to 5815 mm.

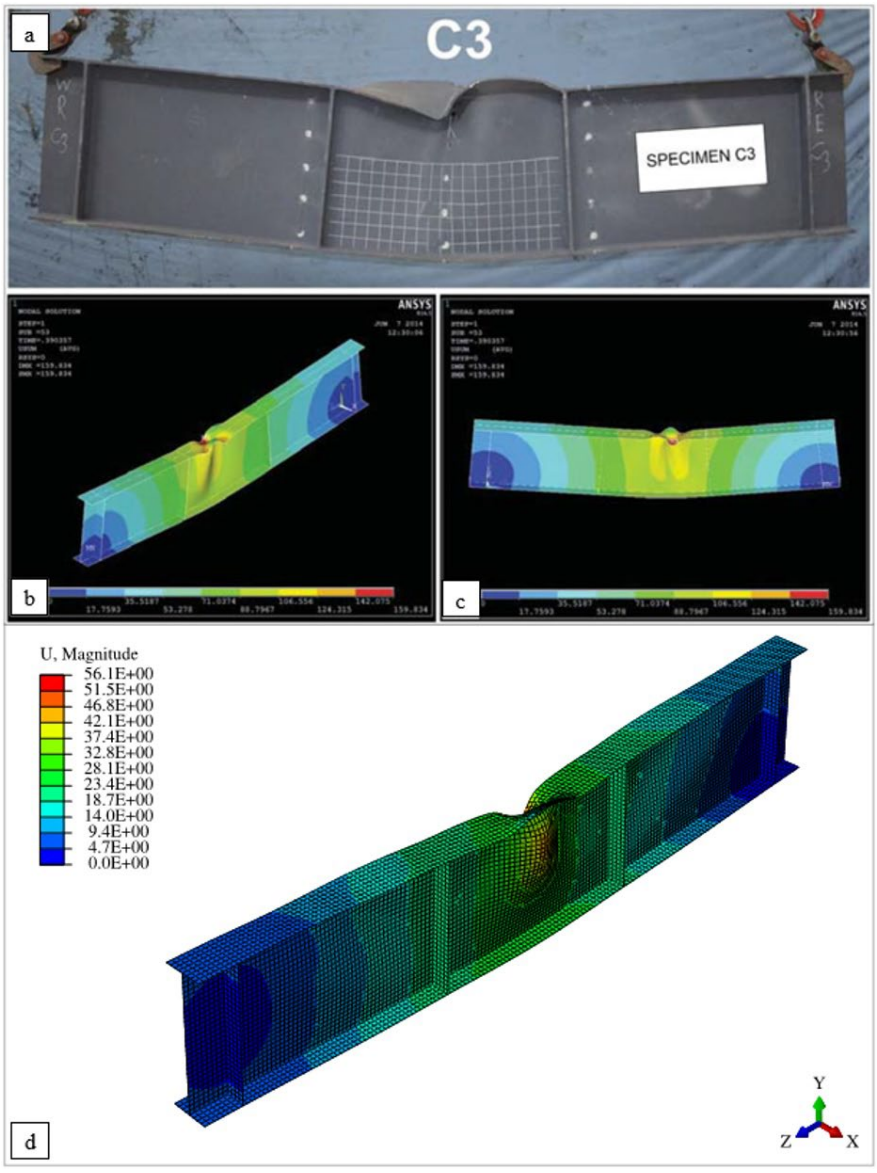

Figure 5: Finite element model verification for beam C3: (a) Experimental test by Shokouhian (2014), (b) Isometric view of the numerical model by Shokouhian (2014), (c) Front view of the numerical model by Shokouhian (2014) and (d) Isometric view of the proposed numerical model (adapted from Shokouhian, 2014).

Table 3 presents the dimensions of the flanges, webs and rectangular longitudinal stiffeners considered in the mean plane of the cross section of the two analyzed panels, where b_{fb} is the width of the lower flange; b_{fu} is the width of the upper flange; h' is the height of the web considering the mean plane of the cross section; t_{fb} is the thickness of the

bottom flange; t_{fu} is the thickness of the upper flange; t_w is the thickness of the web; b_{sl} is the width of the rectangular longitudinal stiffener and t_{sl} is the thickness of the rectangular longitudinal stiffener.

Table 3: Dimensions of the panels considered for the analyses.

Panel	h' (mm)	t_w (mm)	a (mm)	b_{fu} (mm)	t_{fu} (mm)	b_{fb} (mm)	t_{fb} (mm)	b_{sl} (mm)	t_{sl} (mm)
SO	1520.285	7.180	1498.200	320.900	22.290	318.700	22.280	90.000	9.800
UO	1818.010	5.900	1797.500	249.500	20.010	451.200	20.010	100.100	10.230

From the author's experimental results, true curves of stress versus strain were determined. Steel has f_y = 355.00 N/mm^2, longitudinal modulus of elasticity (E) = 210.00 GPa and Poisson coefficient (υ) equal to 0.3. In Figure 6, it is possible to observe the behavior and values of each of the plates used both in the model with a rectangular longitudinal stiffener and in the model with two rectangular longitudinal stiffeners.

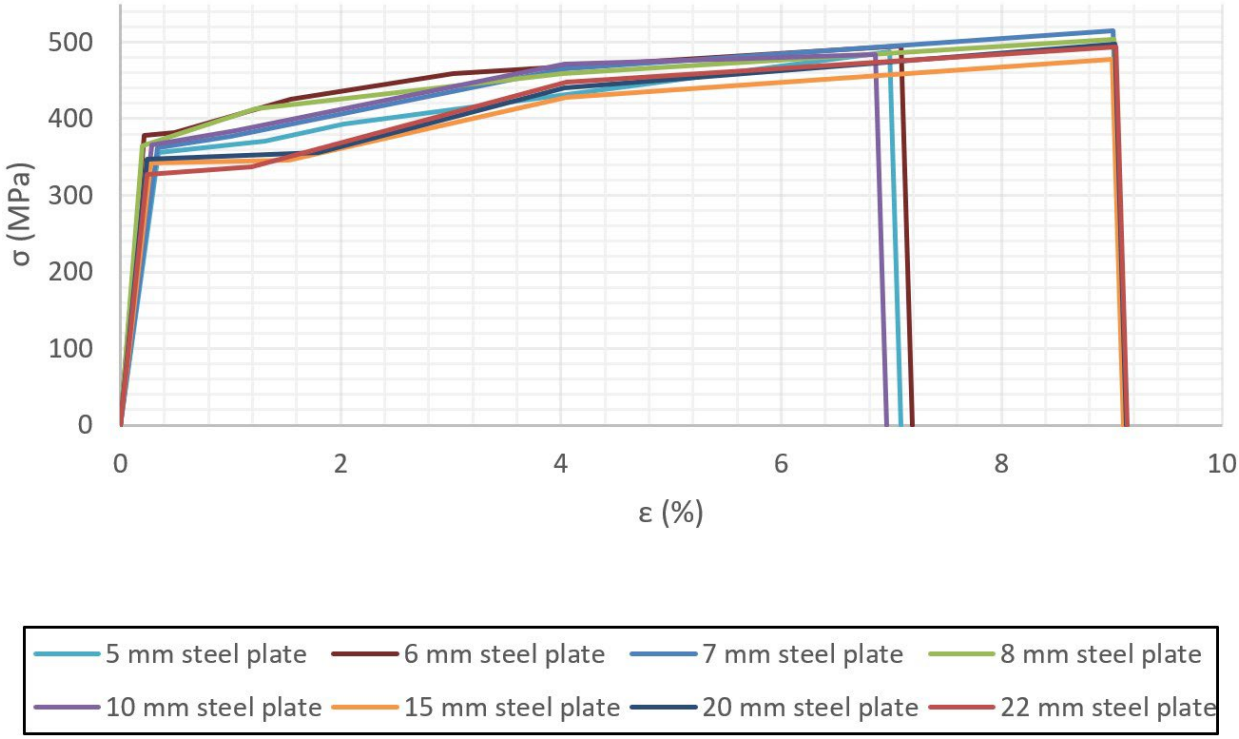

Figure 6: Stress x elastic-plastic strain diagram adopted in the analysis of slender models (adapted from Sinur, 2011).

In Figures 7 and 8 it is possible to visualize the dimensions of the two beams, the application of the load and the lateral restriction in the analyzed panels.

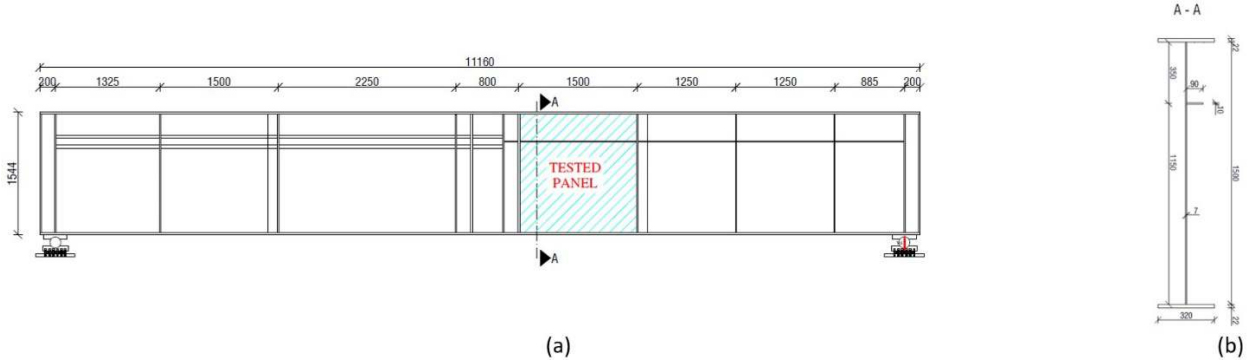

Figure 7: Symmetric beam: (a) Geometric specification of the numerical model for analysis of the SO panel and (b) Detailing of the A-A section of the analyzed panel (Sinur, 2011).

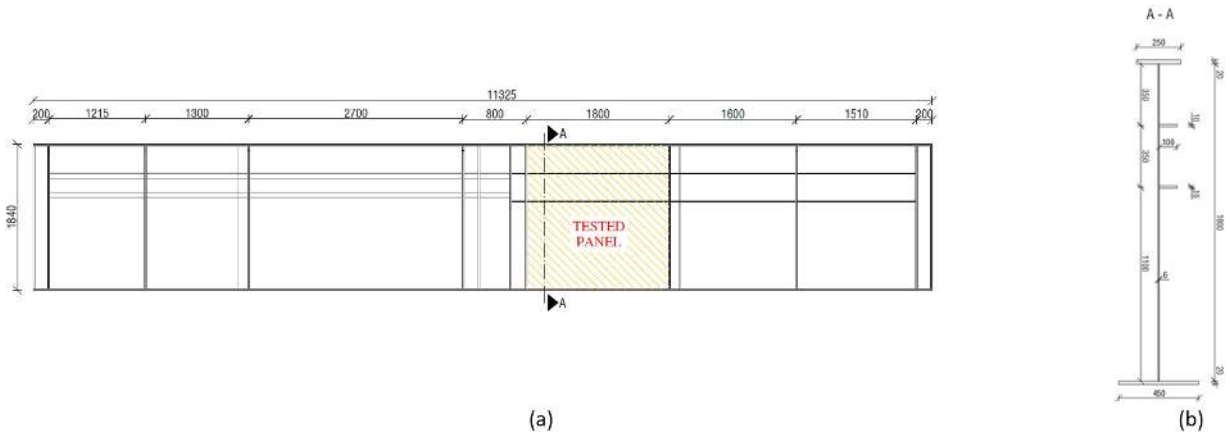

Figure 8: Asymmetric beam: (a) Geometric specification of the numerical model for analysis of the UO panel and (b) Detailing of the A-A section of the analyzed panel (Sinur, 2011).

For the slender model, the same boundary conditions and the same average dimension of the finite elements of the compact model were utilized. The objective of the research is to find a single numerical model that is capable of representing compact and slender laterally constrained beams subjected to bending. However, in the case of slender panels, the load was applied on a rigid circular solid which has a diameter of 200 mm and a thickness of 60 mm. Regarding the initial geometric imperfections, the same procedure was performed as for the compact beams, but in the case of the slender beams, the imperfection adopted throughout the model was equal to the largest displacement outside the panel plate for the first failure mode, obtained through photogrammetry by the authors.

3 RESULTS

After analyzing the ultimate strength capacity of the compact beams, another analysis between the normalized moment (M/M_p) and the normalized rotation of the joint at the end of the beam (θ/θ_p) was conducted to express the bending behavior of the beams. Figure 9, Figure 10 and Figure 11 depict the comparison between the results obtained in this study (solid line) and the experimental (dot line) and numerical (dash-dot line) results obtained by Shokouhian (2014).

Taking into account the analysis of the ultimate resistance moments obtained, it was observed that, for most beams, the numerical model adopted reached results that were sufficiently close, both to the numerical model and to the experimental model proposed by Shokouhian (2014). However, for beam H2, the relative error was greater than 10%. This can be explained by the fact that H2 is the only beam that has 800 mm of distance between the concentrated forces – all other beams have a distance of 1000 mm and this may have confused the author when calculating material properties. Even so, the error was around 16%, which was considered an acceptable error in view of the uncertainties of the model, due to the lack of more information.

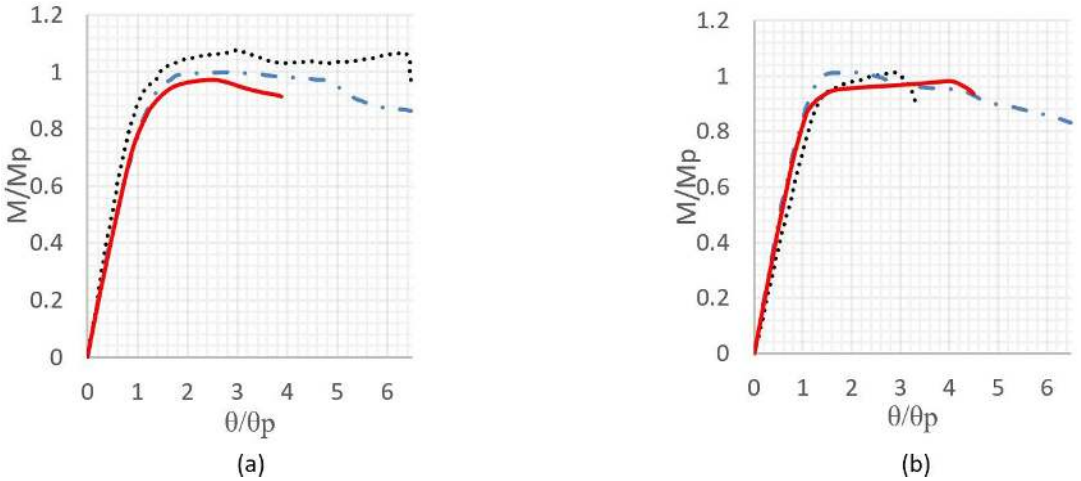

Figure 9: Comparison between bending moment and rotation: (a) Beam C1 and (b) Beam H1 (adapted from Shokouhian, 2014).

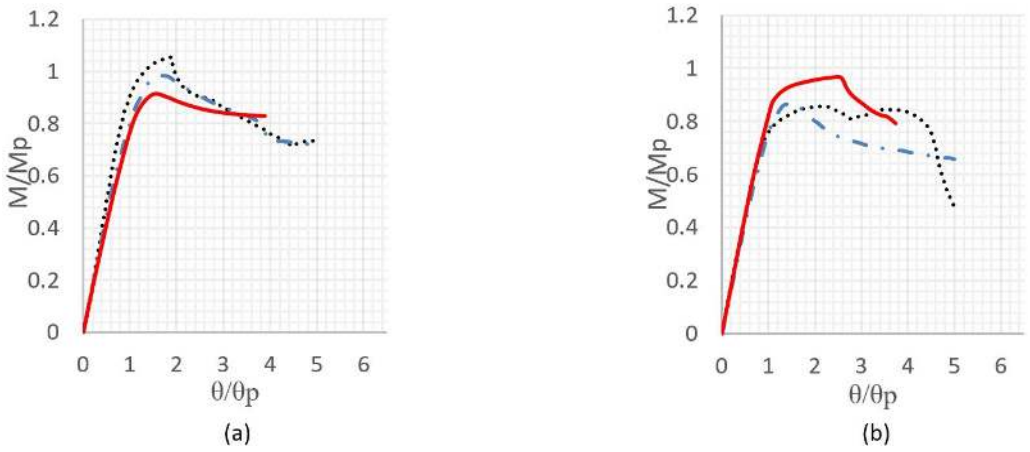

Figure 10: Comparison between bending moment and rotation: (a) Beam C2 and (b) Beam H2 (adapted from Shokouhian, 2014).

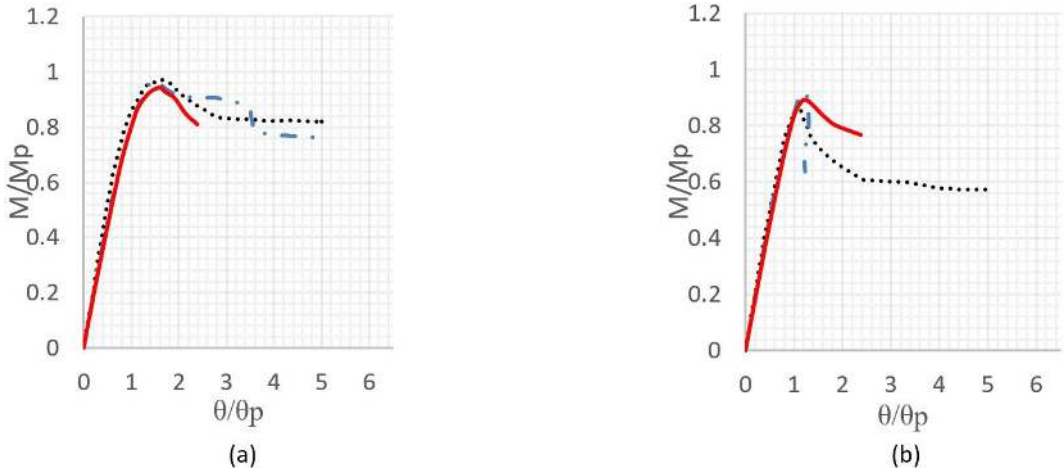

Figure 11: Comparison between bending moment and rotation: (a) Beam C3 and (b) Beam H3 (adapted from Shokouhian, 2014).

Furthermore, as shown in Table 4, it is possible to conclude that, for these cases, the strength capacity of hybrid beams is around 14% to 28% greater than that determined for conventional beams. The result obtained is expected, considering the use of steels with greater resistance in hybrid beams, which lead to an increase in the strength capacity.

Table 4: Comparison of ultimate resistance between researches.

Model	$P_{ul\ (FE\ Model\ proposed)}$ (N)	$P_{ul\ (Experiment-\text{Shokouhian})}$ (N)	$P_{ul\ (FE\ Model-\text{Shokouhian})}$ (N)
C1	416875.38	447940.17	414282.33
C2	549032.44	616742.33	575275.75
C3	804235.49	784882.46	788115.76
H1	530868.10	546161.28	546700.43
H2	711872.17	615085.58	621522.52
H3	921827.77	879891.82	936921.85

Regarding the slender panels, an analysis of the force versus vertical displacement curves was conducted, as can be seen in Figure 12. In Figures 13 to 15, it is observed the evolution of the out-of-plane displacement and the von Misses stress in the SO panel: (a) results of the experimental model for vertical displacements of 20.18 mm, 30.18 mm, 45.18 mm and 55.18 mm, respectively (Sinur, 2011) and (b) results of the numerical model proposed for vertical displacements of 22.70 mm, 30.03 mm, 44.98 mm and 54.07 mm, respectively.

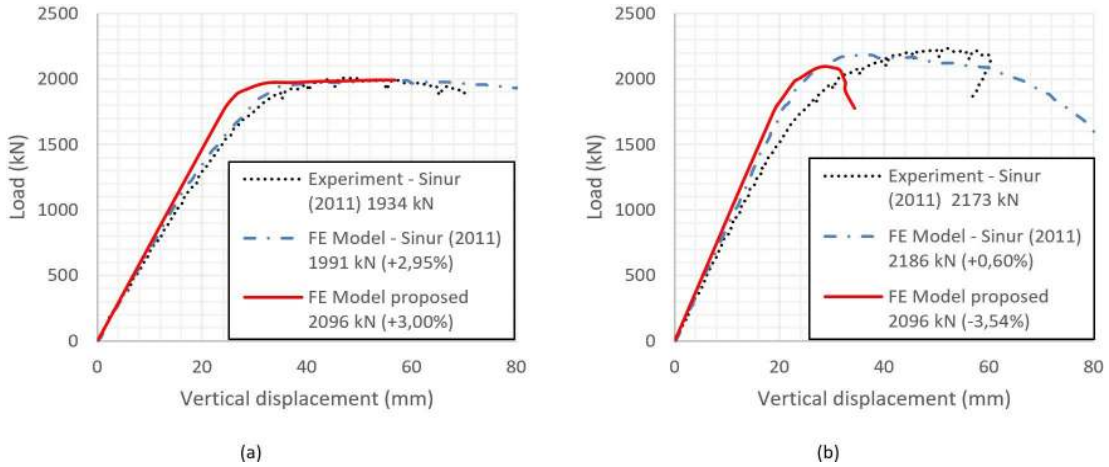

Figure 12: Comparison of load versus vertical displacement curves: (a) SO panel and (b) UO panel

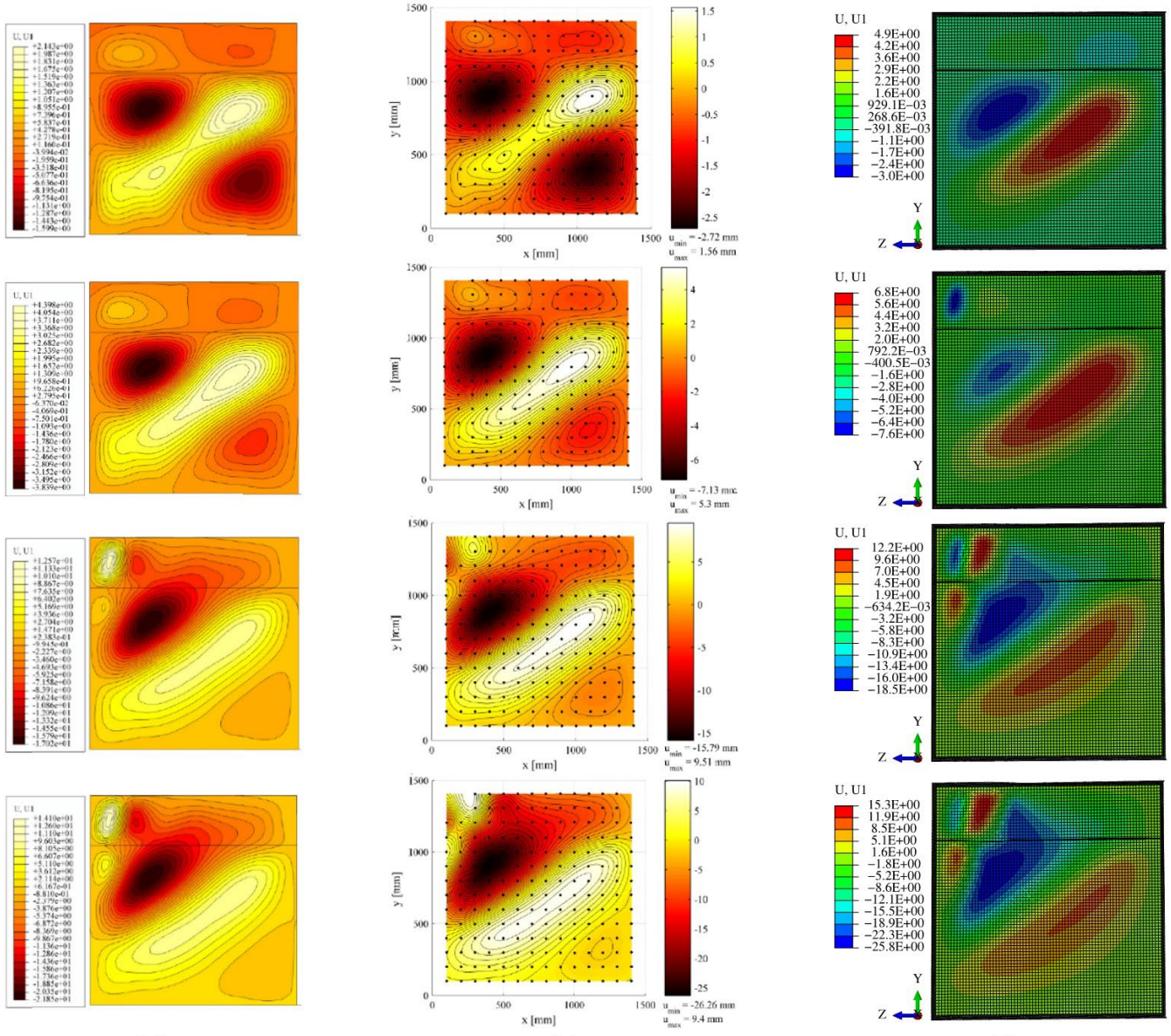

Figure 13: Evolution of the out-of-plane displacement in the SO panel: (a) results from the numerical model (Sinur, 2011), (b) results from the experimental model (Sinur, 2011) and (c) results from the proposed numerical model.

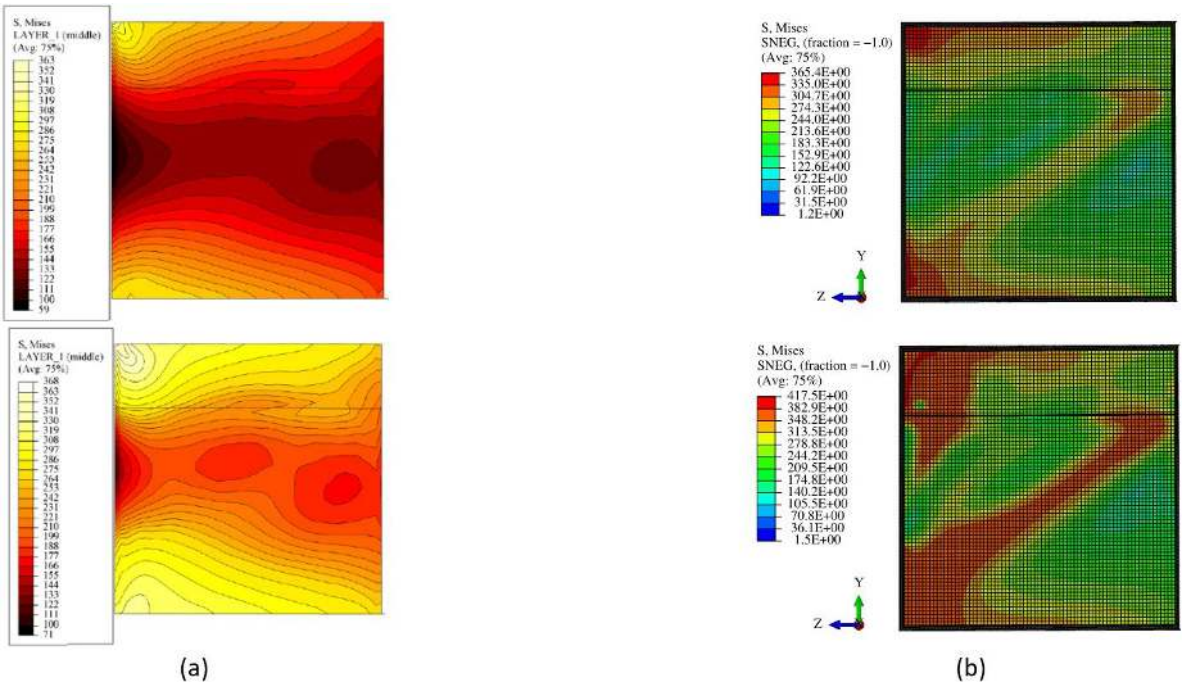

Figure 14: Evolution of the von Misses stress in the SO panel: (a) results from the numerical model (Sinur, 2011) and (b) results from the proposed numerical model (continued)

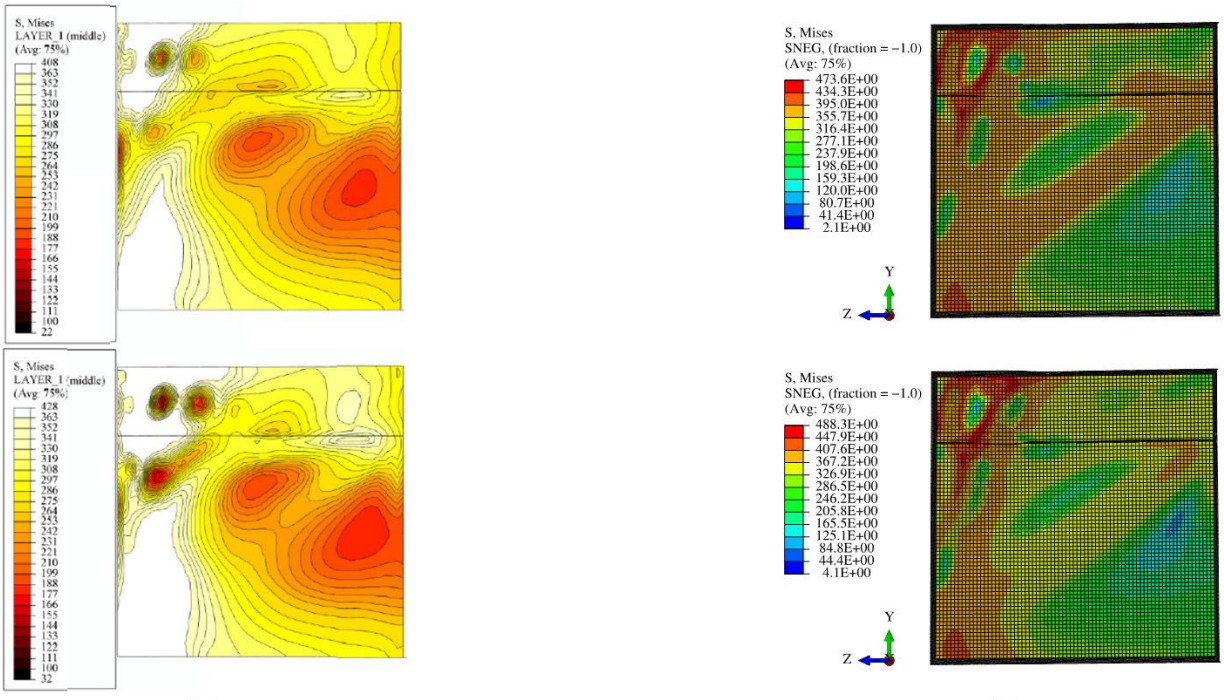

Figure 15: Evolution of the von Misses stress in the SO panel: (a) results from the numerical model (Sinur, 2011) and (b) results from the proposed numerical model (conclusion).

A good agreement was obtained between the author's experimental and numerical research and the numerical results of the proposed model. Furthermore, when comparing the ultimate strengths obtained in the proposed model to the ultimate strength according to EN 1993-1-5, $F_{EN\ 1993-1-5} = 1792\ kN$ for the SO panel and $F_{EN\ 1993-1-5} = 1746\ kN$ for the UO panel. This means that, regarding ultimate loads, the proposed model presented a relative error of less than 4% in both cases when compared with the author's experimental results. The author's numerical results showed a difference of 11.10% and 25.20% for the SO and OU panels, respectively, which are quite similar to the results obtained from the proposed model, which were 11.16% and 20.05%, respectively.

The failure modes are also similar and the evolution of out-of-plane displacement and von Misses stress in the analyses also showed a convergence with the author's results. The biggest divergence is in the out-of-plane displacements observed in the UO panel as a consequence to the vertical displacements, which explains why the numerical model discontinued earlier than expected. The explanation for this event is also one of the guidelines of Sinur's (2011) research, as in his study of mesh convergence it was detected that out-of-plane displacements are the most sensitive parameter of the analysis. Therefore, the proposed model behaved satisfactorily.

In addition, the influence of the variation in the yield strength of the flanges and the web on the behavior of compact beams, symmetrical slender panels with a longitudinal rectangular stiffener and asymmetrical slender panels with two longitudinal rectangular stiffeners was analyzed. For slender panels, the f_{yf}/f_{yw} ratio must not exceed a value of 2.0, which is the limit recommended for the study of hybrid beams.

Thus, beam C3 of the compact model and the panels SO and OU were analyzed in this chapter. In addition, the structural steel classes mentioned in the previous paragraph were utilized. It was assumed that the class numeral is the minimum yield limit. The elasto-plastic behavior of structural steels was considered and the longitudinal modulus of elasticity (*E*) = 200 GPa and the Poisson coefficient (*υ*) equals to 0.3. The deformation of the sections was defined according to the research of Almeida (2012) so that the deformation $10\varepsilon_y$ defines the end of the yield plateau, which was assumed equal to $1{,}01f_y$ and the ultimate stress (f_u) corresponds to $100\varepsilon_y$. With regard to imperfections, the same distribution of residual stresses as Castro and Silva (2006) was utilized and the geometric imperfection equal to L/1500 was assumed. Table 5 presents the results of the ultimate strengths of beam C3 and the compositions of each of the models.

Most models resulted in a difference of 6.00% at most, when compared to the resistance moment results. Only model 5 showed a difference of 19.07%, which can be explained by the fact that the f_{yf}/f_{yw} ratio is very close to the recommended limit for the study of hybrid beams. Figure 16 depicts the results of the ultimate strengths of UO and SO panels.

As expected, in Figure 17 it is shown that in the hybrid section the yield begins in the fiber furthest from the web. For this analysis, f_{yw} = 235,58 MPa.

Table 5: Comparison of ultimate strength between beam C3 analyses.

Model	Structural steel classes		$M_{ul\,(FE\ Model\ proposed)}$ (kNm)	$M_{p\,(theoretical)}$ (kNm)
	Web and stiffeners	Flanges		
1	S235	S235	454.79	467.47
2	S355	S355	677.37	706.18
3	S460	S460	864.96	915.05
4	S235	S355	583.87	617.46
5	S235	S460	605.92	748.71
6	S355	S460	801.79	837.42

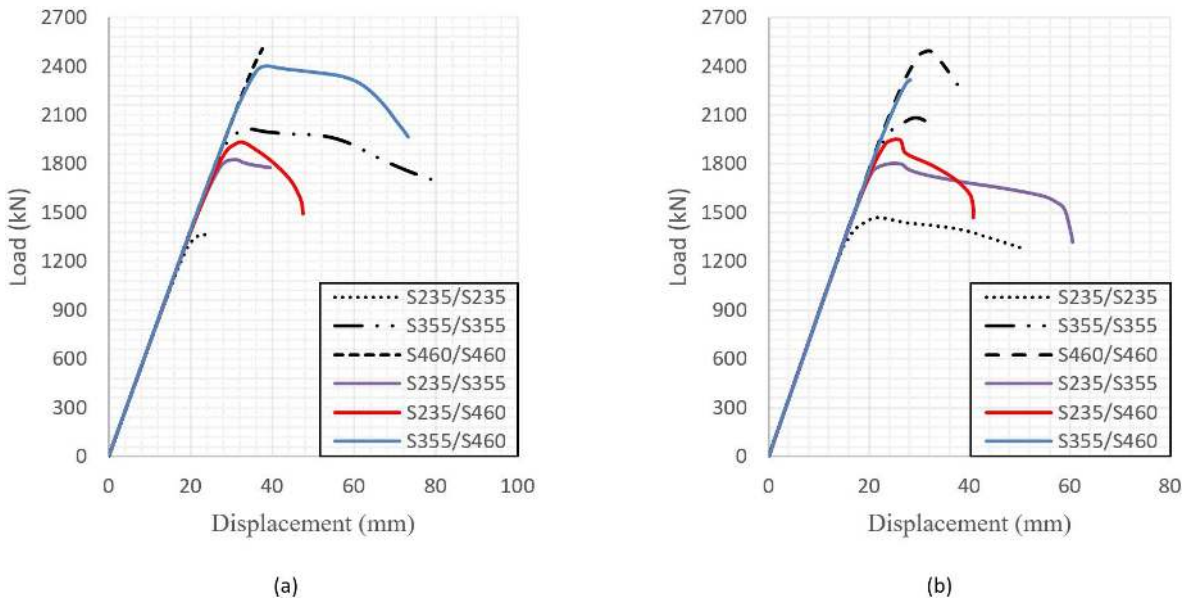

Figure 16: Load versus displacement according to the utilized steel classes: (a) SO panel and (b) UO panel.

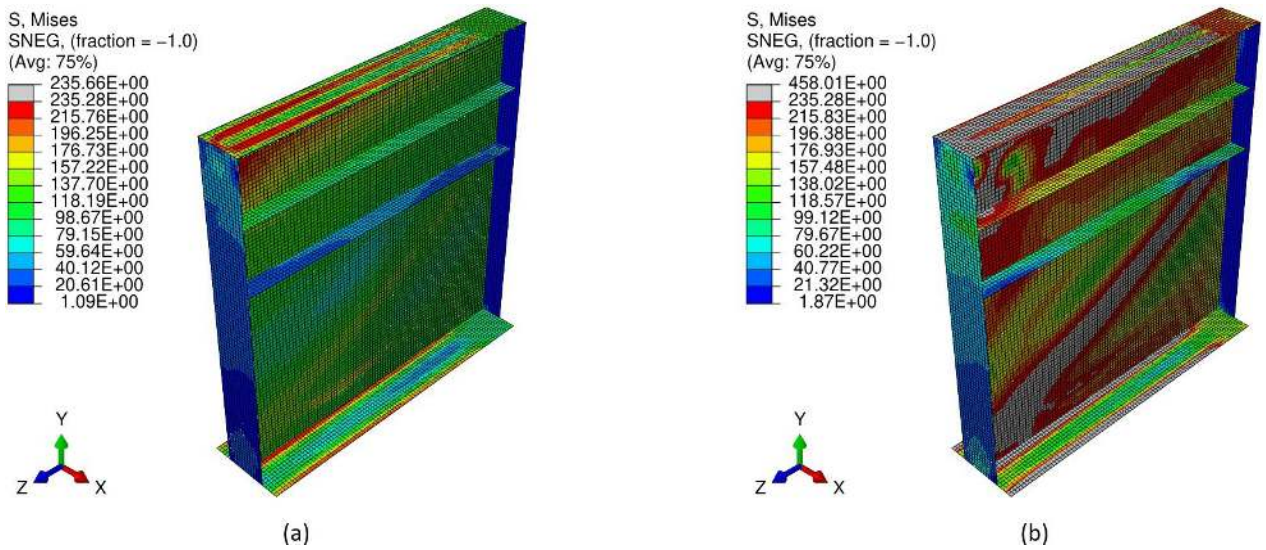

Figure 17: Von Mises stresses: (a) homogeneous UO panel and (b) hybrid UO panel.

4 CONCLUSION

In this article a numerical study was carried out based on simply supported beams contained laterally with I-profile bended in relation to the axis of greatest inertia. The validation of the three numerical models based on the Finite Element Method was elaborated in the commercial software ABAQUS. The first model refers to compact beams from the study by Shokouhian (2014) and the other two relate to slender panels with one and two longitudinal stiffeners from the study by Sinur (2011). The three numerical models have the same load application characteristics, boundary conditions, etc. so that it would be possible to achieve a single general model for beams and panels.

In comparison to the research on compact beams by Shokouhian (2014), the proposed numerical model is in accord with the failure modes obtained by the author. Regarding the ultimate resistance moments, the results obtained were very close to those of Shokouhian (2014) for most analyzed beams. Exclusively in the analysis of beam H2, a relative error of 16% was calculated, which can be explained by the difference in the geometry of this beam. With this research it was concluded that the strength capacity of the hybrid beams is around 14% to 28% greater than those determined for the conventional beams.

The numerical model for the proposed slender panels was compared to the results of Sinur (2011). The SO panel has a symmetrical cross section with one rectangular stiffener and the UO panel has an asymmetrical cross section with two rectangular stiffeners. As a result, a relative error of less than 4% was obtained in both cases regarding the ultimate loads. In addition, the deformations, the evolution of out-of-plane displacement and von Mises stress coincides with the author's results. It is noted that there was a greater divergence related to out-of-plane displacements obtained in the analysis of the UO panel, which is explained by the fact that out-of-plane displacements are the most sensitive parameter of the analysis.

Lastly, this research fulfilled the proposed objectives and resulted in the development of a numerical model capable of representing compact and slender beams subjected to bending.

Acknowledgment

The authors would like to thank CAPES (Coordination for the Improvement of Higher Education Personnel), CNPq (National Council for Scientific and Technological Development), FAPEMIG (Foundation for Research Support of the State of Minas Gerais) and UFMG (Federal University of Minas Gerais).

Author's Contribuitions: Conceptualization, CM Calisto; Methodology, CM Calisto; Investigation, CM Calisto; Writing - original draft, CM Calisto; Writing - review & editing, CM Calisto, ALRC Silva, RB Caldas and H Carvalho; Supervision, ALRC Silva, RB Caldas and H Carvalho.

Editor: Pablo Andrés Muñoz Rojas

References

AASHTO LRFD Bridge Design Specifications. (2014). Washington: American Association of State Highway and Transportation Officials.

Abuyounest, S., Adeli, H. (1987). Optimization of hybrid steel plate girders. Computers & Structures, 27, 575-582.

Adeli, H., Phan, K. (1986). Interactive computer-aided design of non-hybrid and hybrid plate girders. Computers & Structures, 22, 267-289.

Ajeesh, S. S. (2011). Shear Resistance of Hybrid Plate Girder. INSDAG'S STEEL IN CONSTRUCTION, 12, 33-44.

Axhag, F. (1998). Plastic design of slender steel bridge girders. Doctoral Thesis. Luleå University of Technology.

Azizinamini, A., Hash, B., Yakel, A. J., and Farimani, R. (2007). Shear Capacity of Hybrid Plate Girders. Journal of Bridge Engineering - ASCE, 535-543.

Ban, H., Shi, G., Bai, Y., Shi, Y., and Wang, Y. (2013). Residual Stress of 460 MPa High Strength Steel Welded I Section: Experimental Investigation and Modeling. International Journal of Steel Structures, 691-705.

Barker, M. G. (2005). Shear Tests of High Performance Steel Hybrid Girders.

Barker, M. G., Schrage, S. D. (2000). High-Performance Steel Bridge Design and Cost Comparisons. Transportation Research Record, 33-39.

Barth, K. E., Righman, J. E., and Freeman, L. B. (2007). Assessment of AASHTO LFRD Specifications for Hybrid HPS 690W Steel I-Girders. Journal of Bridge Engineering - ASCE.

Barth, K. E., Yang, L., and Righman, J. (2007). Simplified Moment Redistribution of Hybrid HPS 485W Bridge Girders in Negative Bending. Journal of Bridge Engineering - ASCE, 456-466.

Beg, D., Kuhlmann, U., Davaine, L., and Braun, B. (2010). Design of Plated Structures. ECCS - European Convention for Constructional Steelwork.

Biscaya, A., Pedro, J. O., and Kuhlmann, U. (2019). Experimental and numerical studies on the M-V-N interaction of longitudinally stiffened steel I-girders. Annual Stability Conference Structural Stability Research Council. St. Louis, Missouri.

Castro e Silva, A. L. (2006). Análise numérica não linear da flambagem local de perfis de aço estrutural submetidos à compressão uniaxial. Belo Horizonte: Tese de Doutorado.

Chacón, R. F. (2009). Resistance of Transversally Stiffened Hybrid Steel Plate Girders to Concentrated Loads. 235. Barcelona: Doctoral Thesis.

Chacón, R. F. (2014). Vigas armadas híbridas de acero. Estado del conocimiento. Revista Ciencia e Ingeniería, 95-102.

Chacón, R., Bock, M. R. (2011). Longitudinally stiffened hybrid steel plate girders subjected to patch loading. Journal of Constructional Steel Research, 1310-1324.

Chacón, R., Mirambell, E. R. (2010). Hybrid steel plate girders subjected to patch loading, Part 1: Numerical study. Journal of Constructional Steel Research, 695-708.

Chacón, R., Mirambell, E. R. (2010). Hybrid steel plate girders subjected to patch loading, Part 2: Design proposal. Journal of Constructional Steel Research, 709-715.

Chacón, R., Mirambell, E. R. (2013). Transversally stiffened plate girders subjected to patch loading. Part 1. Preliminary study. Journal of Constructional Steel Research, 483-491.

Chacón, R., Rojas-Blonval, J. E. (2015). Evaluación de la resistencia a abolladura por cortante de vigas armadas híbridas de acero según la norma venezolana COVENIN 1618:1998. Informes de la Construcción, 67.

Chacón, R., Bock, M., Mirambell, E., and Real, E. (2012). Hybrid steel plate girders subjected to path loading. Steel Construction, 3-9.

COMBRI. (2008). Competitive steel and composite bridges by innovative steel-plated structures. European Commission.

Eurocode 3 - Design of steel structures - Part 1-1: General rules and rules for buildings. (2005).

Eurocode 3 - Design of steel structures - Part 1-12: Additional rules for the extension of EN 1993 up to steel grades S700. (2007).

Eurocode 3 - Design of steel structures - Part 1-5: Plated structural elements. (2006).

Filho, J. O. P., Tankova, T., Carvalho, H., Martins, C. and Simões da Silva, L. (2022). Experimental and numerical flexural buckling resistance of high strength steel columns and beam-columns. Engineering Structures 265 (1-3): 114414

Fenkel, J. P., Rizos, D. C., and Ziehl, P. H. (2007). Structural performance and design evaluation of HPS 70W bridge girders. Journal of Constructional Steel Research, 909-921.

Ghadami, A., Broujerdian, V. (Advances in Structural Engineering). Flexure-shear interaction in hybrid steel I-girders at ambient and elevated temperatures. 2018, 1-16.

Gogou, E. (2012). Use of High Strength Steel Grades for Economical Bridge Design. Amsterdam: Master Thesis Study.

Greco, N., Earls, C. J. (2003). Structural Ductility in Hybrid High Performance Steel Beams. Journal of Structural Engineering - ASCE, 1584-1595.

Ito, M., Nozaka, K., Shirosaki, T., and Yamasaki, K. (2005). Experimental Study on Moment-Plastic Rotation Capacity of Hybrid Beams. Journal of Bridge Engineering - ASCE.

Johansson, B., Collin, P. (2005). Eurocode for High Strength Steel and Applications in Construction.

Khartode, R. R., Godase, A. A., Narule, G., and Ahiwale D. (2020). A Parametric Study of Hybrid Steel Plate Girder. GIS Science Journal, vol. 7, pp. 1045-1058.

Khartode, R., Nimbalkar, D., Pise, A., Pote, S., Purigosavi, S., Morkhade, S., Ahiwale, D., and Raut, K. (2020). Finite element analysis of hybrid steel welded I section using ANSYS software. Journal of Seybold Report, vol.15, pp. 3138-3146.

Kulkarni, A. S., Gupta, L. M. (2017). Experimental Investigation on Flexural Response of Hybrid Steel Plate Girder. KSCE Journal of Civil Engineering.

Lalthazuala, R., Singh, K. D. (2019). Investigations on structural performance of hybrid stainless steel I-beams based on slenderness. Thin-Walled Structures, 197-212.

Lew, H. S., Toprac, A. A. (1967). Static Tests on hybrid plate girders. Center for highway research, The University of Texas, Austin, Texas.

Maeda, Y. (1971). Additional study on static strength of hybrid plate girders in bending. ETH Library, 409-413.

Rojas-Blonval, J. E. (2013). Vigas híbridas sometidas a solicitaciones de cortante. Tesis de Máster. Universitat Politècnica de Catalunya.

Sarsam, J. B. (1966). Behavior of thin web hybrid beams subjected to static loads. Master Thesis. South Dakota State University.

Shokouhian, M. (2014). Investigation of Ductility and Section Resistance in Hybrid Flexural Members with Q460 High Strength Steel. Doctoral Thesis.

Shokouhian, M., Shi, Y. (2014). Investigation of Ductility in Hybrid and High Strength Steel Beams. International Journal of Steel Structures, 265-279.

Shokouhian, M., Shi, Y. (2015). Flexural strength of hybrid steel I-beams based on slenderness. Engineering Structures, 114-128.

Shokouhian, M., Head, M., and Shi, Y. (2018). A Direct Design Method for Hybrid High Strength Steel Beams Based on Slenderness. Los Angeles, California: Eleventh U.S. National Conference on Earthquake Engineering.

Shokouhian, M., Shi, Y., and Head, M. (2016). Interactive buckling failure modes of hybrid steel flexural members. Engineering Structures, 153-166.

Sinur, F. (2011). Behaviour of Longitudinally Stiffened Plate Girders Subjected to Bending-Shear Interaction. Ljubljana: Doctoral thesis.

Su A, Liang Y, Zhao O. Experimental and numerical studies of S960 ultra-high strength steel welded I-section columns. Thin-Walled Struct 2020;107166.

Subramanian, L., W., W. D. (2016). Flexural Resistance of Longitudinally Stiffened I-Girders. I: Yield Limit State. Journal of Bridge Engineering - ASCE.

Veljkovic, M., Johansson, B. (2004). Design of hybrid steel girders. Journal of Constructional Steel Research, 535-547.

Wang, C. S., Duan, L., Chen, Y. F., and Wang, S. C. (2016). Flexural behavior and ductility of hybrid high performance steel I-girders. Journal of Constructional Steel Research, 1-14.